STRUCTURAL INSIGHTS INTO HEPATITIS C VIRUS RECEPTOR BINDING AND ENTRY

Ashish Kumar[1], **Reafa A. Hossain**[1], **Samantha A. Yost**[2], **Wei Bu**[3], **Yuanyuan Wang**[1], **Altaira D. Dearborn**[1], **Arash Grakoui**[4,5], **Jeffrey I. Cohen**[3], **Joseph Marcotrigiano**[1]

[1]Structural Virology Section, Laboratory of Infectious Diseases, National Institute of Allergy and Infectious Diseases, National Institutes of Health, Bethesda, MD 20892

[2]Center for Advanced Biotechnology and Medicine, Rutgers, The State University of New Jersey, Piscataway, NJ 08854

[3]Medical Virology Section, Laboratory of Infectious Diseases, National Institute of Allergy and Infectious Diseases, National Institutes of Health, Bethesda, MD 20892

[4]Division of Infectious Diseases, Emory Vaccine Center, Division of Microbiology and Immunology, Emory University School of Medicine, Atlanta, GA 30322

[5]Yerkes National Primate Research Center, Emory Vaccine Center, Atlanta, GA 30329

Abstract

Hepatitis C virus (HCV) infection is a causal agent of chronic liver disease, cirrhosis, and hepatocellular carcinoma in humans, afflicting more than 70 million people worldwide. HCV envelope glycoproteins E1 and E2 are responsible for host cell binding, but the exact entry process remains undetermined[1]. The majority of broadly neutralizing antibodies preclude interaction between HCV E2 and the large extracellular loop (LEL) of the cellular receptor CD81[2]. We observed that low pH enhances CD81-LEL binding to E2 and determined the crystal structures of E2/Fab 2A12/CD81-LEL, E2/Fab 2A12, and CD81-LEL. Upon binding CD81, E2 residues 418–422 are displaced, allowing for the extension of an internal loop, residues 520–539. Docking of the E2/CD81-LEL complex onto a membrane embedded, full length CD81 places Tyr529 and Trp531 of E2 proximal to the membrane. Liposome flotation assays demonstrate that low pH and CD81-LEL increase E2 interaction with membranes, while structure-based mutants of Tyr529, Trp531, and Ile422 of the E2 amino terminus abolish membrane binding. These data support a model that acidification and receptor binding result in a conformation change in E2 in preparation for membrane fusion.

Results

HCV enters hepatocytes through a multistep process requiring a series of host cellular factors and the viral envelope glycoproteins E1 and E2 (reviewed in [1]). The HCV glycoproteins mediate cell targeting, endocytosis, and membrane fusion ultimately stimulated by endosomal acidification[3]. At least four cellular factors are critical for HCV attachment and entry: CD81, scavenger receptor class B type I (SRBI), claudin-1 (CLDN), and occludin (OCLN), yet blocking the E2-CD81 interaction is the primary means of antibody-mediated neutralization[2]. CD81 is ubiquitously expressed on a variety of cell lines, indicating a role secondary to hepatocyte-specific receptor binding. CD81 translocates with the virion to tight junctions and engages with late entry factors, CLDN and OCLN, in the endosome for acidification and entry. CD81 is an integral membrane protein of the tetraspanin family containing four transmembrane helices. The CD81 large extracellular loop (LEL), a globular domain made of five helices (A–E), binds E2 and residues that are essential for the interaction have been previously identified[4–9]. The molecular mechanisms thereafter, for mediating cell entry and membrane fusion for HCV, remain undefined.

Initial crystallization trials demonstrated the presence of low pH as a critical determinant for crystal formation, therefore the affinity of human and tamarin CD81-LEL (hCD81-LEL and tCD81-LEL, respectively) for the ectodomain of E2 (eE2) was measured at neutral and low pH. Differing from human CD81 by only five amino acids (Extended Data Figure 1), tamarin CD81 supports HCV infection and binds E2 more effectively[10,11]. tCD81-LEL showed a four-fold increase in affinity of for ectodomain E2 (eE2) versus hCD81-LEL (175 nM and 773 nM, respectively) (Extended Data Table 1 and Extended Data Figure 2). Low pH (5.0) increased the affinity of tCD81-LEL for eE2 4.7-fold (175 nM at pH 7.5 to 37 nM at pH 5.0) while hCD81-LEL showed only a modest 1.1-fold increase (773 nM at pH 7.5 to 681 nM at pH 5.0) (Extended Data Table 1 and Extended Data Figure 2). A low pH complex of tCD81-LEL/ HVR1-eE2 (deletion of the hypervariable region 1 of eE2) with a non-neutralizing antibody (non-NAb) Fab, 2A12[12], as a crystallization chaperone, yielded crystals that diffracted to about 3.3Å resolution. To assist in the identification of changes upon complex formation, structures of full-length, fully glycosylated eE2/2A12 as well as tCD81-LEL alone were also determined (Figure 1 and Extended Data Table 2).

Conformational changes in E2 and CD81

The tCD81-LEL/ HVR1-eE2/2A12 structure has two complexes in the asymmetric unit, permitting two independent observations of the interaction (Figure 1A and Extended Data Figure 3). The non-crystallographic, two-fold symmetry axis resembles the homodimer observed in the tCD81-LEL structure (Figure 1C) and previously reported hCD81-LEL structures[13,14], and is likely a biochemical artifact as the interface clashes with the transmembrane helices (TM) of the full-length CD81 structures[15,16]. Each tCD81-LEL is bound to a copy of HVR1-eE2, and each HVR1-eE2 is, in turn, bound to a 2A12 Fab. There are no contacts between the E2 molecules in the asymmetric unit (Extended Data Figure 3) but the complexes are highly similar with an alpha carbon root mean squared deviation (R.M.S.D.) of 1.0Å.

The overall structure of E2 in the eE2/2A12 and tCD81-LEL/ HVR1-eE2/2A12 complexes (Figure 1A and 1B) is similar to previous reports[12,17,18,19,20]. We observed two noteworthy conformational changes in residues 418–422 and 520–539 (CD81-binding loop) of E2 (Extended Data Figure 4 and Figure 1A, B, and D). In the absence of CD81, residues 384–421 (HVR1 and antigenic site 412) of eE2 are disordered, while the CD81-binding loop is packed against residues 422–427 (Figure 1B, 2A and B, and Extended Data Figure 4). The tip of the CD81-binding loop (represented by Tyr529) interacts with Ile422 (Figure 2B). In the presence of tCD81-LEL, residues 418–421 become ordered and wrap around CD81 with Ile422 moving >9Å (Figure 2B). The CD81-binding loop extends a dramatic 13–15Å to pack partly against tCD81-LEL (Figures 1A, 2A and B). The CD81-binding loop adopts a similar conformation in each complex in the asymmetric unit (Extended Data Figure 5). CD81 binding appears to stabilize an alternate conformation of residues 418–427, including Ile422, allowing for loop extension (Figure 2B). This mechanism is supported by our previous structure of the E2 core wherein the 520–539 loop was disordered due to the deletion of 384–455, including Ile422[12].

Previous hCD81-LEL structures were classified into 'open', 'intermediate', and 'closed' conformations based on the relative orientations of the C and D helices (residues 160–188; Figure 2C)[14]. The vast majority of the described hCD81-LEL structures are in the 'closed' conformation, including the LEL from the full-length structure of hCD81[14,21]. The D helix in each tCD81-LEL molecule is unwound in the tCD81-LEL/ HVR1-eE2/2A12 complex structure, adopting instead an extended, open conformation, consistent with flexibility observed in this region using NMR[22] (Figure 2D). Furthermore, in the structure of tCD81-LEL alone the two molecules in the asymmetric unit, adopt an intermediate conformation with a D helix and an extended, open conformation, respectively (Figure 1C and 2D). This open conformation is distinct from the open conformation of hCD81 when bound to CD19, wherein helices D and E join the fourth transmembrane helix as a contiguous structure and half of helix C is unwound[16]. The five amino acid differences between human and tamarin CD81 were mapped in their relation to the E2-binding site (Extended Data Figure 1B). Of the five differences, only T163S and N180S contribute to the CD81/E2 interface, while D155N, V169M, and D196E are directed away from E2. The enhanced affinity between E2 by tCD81 may be due to tCD81-LEL adopting an extended open conformation needed for E2 binding and/or these contact differences.

Neutralizing antibody/CD81 competition

The CD81-binding site on E2 is discontinuous, comprising the antigenic site (AS) 412 epitope and front layer (residues 412–445), the central CD81-binding loop, and residues 616–617 of the back layer (Figure 3; Extended Data Figures 4 and 6; and Extended Data Table 3). The two tCD81-LEL/ HVR1-eE2 complexes in the asymmetric unit have 872Å^2 and 959Å^2 of buried surface with an R.M.S.D. of 1.1Å for similar alpha carbon positions, suggesting binding tolerance in the interface. In both tCD81-LEL/ HVR1-eE2 complexes, eE2 residues Leu441, Phe442, Tyr443, and His445 of the front layer and Tyr617 of the back layer make contact with CD81 (as defined by a distance 4Å, Extended Data Table 3). These residues are highly conserved across HCV genotypes with Leu441, Tyr443 and

Tyr617 being invariant across genotypes. HK6a (genotype 6a) has a lysine at position 445 and SA13 (genotype 5a) has a leucine at 442 (Extended Data Figure 4).

DAO5, a non-NAb recognizes the AS529–540 epitope on the CD81-binding loop distal from CD81, consistent with its inability to neutralize infection (Figure 3A)[23]. A crystal structure of DAO5 bound to a synthetic peptide shows a portion of the CD81-binding loop in an alpha helical conformation, which is not observed in either the retracted or extended form in the eE2 structures. DAO5 is also capable of capturing HCV pseudoparticles, cell culture derived virions (HCVcc), and eE2 in solution[23], suggesting that the CD81-binding loop may be dynamic.

The E2/CD81 interaction is targeted by a series of well-characterized, broadly neutralizing antibodies (bNAbs) and several E2/bNAb structures have been determined[2]. Potent bNAbs isolated from HCV-infected individuals mainly target the overlapping AS412, AS434, and antigenic regions (ARs) (Figure 3A and B). These bNAbs sterically clash with linear and conformational epitopes involved in CD81 binding to E2, indicating that neutralization is accomplished by directly blocking the CD81-binding surface on E2 (Figure 3B, Extended Data Figure 7 and Extended Data Table 3). Superposition of the front and back layers of the published structures of E2/antibody structures onto the E2/CD81 complexed yielded R.M.S.D. ranging from 0.45 to 1.44Å, indicating that receptor and bNAb binding may have slight changes in the conformation of these layers (Figure 3C). All the determined bNAbs/eE2 structures have the CD81-binding loop in the retracted position[12,17,18,19,20].

Superposition onto full length CD81

To provide a better understanding of CD81 binding on HCV entry, each tCD81-LEL/ HVR1-eE2 complex was superimposed onto the full-length, human CD81 structure (PDB ID 5TCX[21]) and docked into an idealized, membrane bilayer. The two planes of spheres represent the carbonyl moieties of the phospholipids and approximate the hydrophobic core of the bilayer (Figure 4A)[24] E2 binds to the edge of CD81 distal from the four transmembrane helices and proximal to the bilayer.

To investigate the effect of charge and pH-sensitive regions in the context of CD81 binding, the electrostatic-potential surfaces of E2 and CD81 were calculated for both the bound and free forms at pH 7.5 and 5.0 (Extended Data Figure 7). The electrostatic surface of eE2/ tCD81-LEL interface does not show a marked change upon lowering the pH (Extended Data Figure 7A, B, E, and F). Protonation of histidine side chains upon endosomal acidification can actuate protein conformational changes in other viral fusion proteins[25]. E2 His421 and His445 are within 4Å of CD81 (Extended Data Table 3), but far from the extended loop of E2. These observations are consistent with a previous proposal that the protonation state of His445 of E2 is a key regulator of the low-pH-dependent fusion mechanism employed by HCV[26]. In fact, use of a lysine in the HCV HK6a strain retains a positive charge at this position (Extended Data Figures 4 and 6). The electrostatic surface of the eE2/CD81-LEL complex is basic and becomes more so upon lowering the pH (Extended Data Figure 7C and D). The superposition model places half of the basic surface of eE2 proximal to the negatively charged membrane while the other half wraps around to the side of complex

(Figure 4B). More studies are needed to clarify the function of the extended form of the E2 loop and pH sensing during HCV infection.

In each complex of the asymmetric unit, the CD81-binding loop extends away from E2 towards the bilayer. Tyr529, Trp531, and Gly532, located at the tip of the loop, are invariant among the major genotypes (Extended Data Figure 4) and are critical for CD81-binding and virus entry[4,7]. The side chains of Tyr529 and Trp531 are oriented towards the outer leaflet of the membrane at distances of <5Å and <10Å from the idealized phosphatidyl carbonyl layer, respectively (Figure 4A). The hydrophilic head groups of the phospholipids would extend ~3-5Å from the hydrophobic core, placing Tyr529 in contact with the membrane. Given the inherent flexibility of both the CD81-binding loop and the membrane bilayer, it would be energetically favorable to insert the side chains of Tyr529 and Trp531 into the outer leaflet of the membrane. The intervening residue at position 530 is not conserved within the different HCV genotypes but is generally polar, which may serve to orient the loop relative to the lipid head groups.

To evaluate the impact of pH, tCD81-LEL, and select E2 mutations on membrane binding, liposome flotation was used as described previously[27]. eE2 Y529A and W531A have greatly reduced hCD81 binding and I422A retains about 50% binding, but each is recognized by conformational antibodies, suggesting that they are correctly folded[4,28]. Wild-type eE2 was incubated with liposomes in the presence or absence of tCD81-LEL at either pH 7.5 or pH 5.0, separated in a sucrose gradient, and detected by E2-specific Western blot (Figure 4C). Liposome-bound proteins migrate to the top of the gradient while free proteins remain at the bottom. Wild-type eE2 demonstrated weak membrane binding at pH 7.5, which improved slightly in the presence of tCD81-LEL. Lowering the pH to 5.0 increased liposome binding, which was enhanced further in the presence of tCD81-LEL. The partial floatation of eE2 is consistent with previous results[27] and is likely due to the small hydrophobic exposed surface formed by Tyr529 and Trp531 (Figure 4B). During HCV entry, insertion of the loop would be assisted by the membrane embedded, full-length CD81. eE2 mutants (I422A, Y529A, W531A, and Y529A/W531A) exhibited <10% liposome binding relative to wild-type eE2 at pH 5.0 in the presence of tCD81-LEL (Figure 4C, D, Extended Data Figure 8). Doubling the amount of mutant eE2 proteins per flotation assay failed to enhance membrane floatation (Extended Data Figure 8). Liposome binding by these mutants was dramatically lower than CD81-independent liposome binding by the wild-type eE2 at pH 7.5 (Figure 4C). Thus, while these E2 mutations are important for CD81 binding and do not noticeably misfold the protein, their impact on liposome binding cannot be attributed solely to reduced CD81 binding.

Discussion

Viral membrane fusion involves a two-step mechanism: priming (e.g. proteolysis) and triggering (e.g., acidification and/or receptor binding)[29]. Once triggered, the trimeric viral glycoprotein introduces a fusion loop or peptide into the cellular membrane, followed by a conformational rearrangement drawing the two membranes together. HCV entry involves cell-type recognition and binding, translocation to the tight junctions, and membrane fusion to the endosome. HCV fusion requires both E1 and E2 glycoproteins as well as low pH

and is primed by CD81-LEL[27]. Thus far, there is little evidence of an eE2 trimer, although the E2 stem, transmembrane helix, or E1 may influence oligomerization. Structural data provided here demonstrate a mechanism by which HCV E2 binds to cellular receptor CD81 at low pH, resulting in the extension of an internal E2 loop towards the endosomal membrane. A fusion loop for HCV has yet to be identified, but the CD81-binding loop displays many necessary characteristics (i.e., membrane binding, low pH trigger, and CD81-dependent extension). Furthermore, there is some additional evidence that a fusion loop may exist in E1 (residues 264-294)[30]. For fusion to occur, a conformational change must bring the viral, membrane-embedded transmembrane helix at the carboxyl terminus of E2 into contact with the host membrane, a distance of 35Å proposed in our docking model (Figure 4A). The intervening stem region of E2, omitted in this study, could span this distance and warrants further investigation. Together, our results show that during entry, E2 employs a hybrid triggering mechanism, wherein both acidification and CD81 interaction are necessary for optimal membrane binding.

Methods

Construct design, expression, and purification of HVR1-eE2, eE2, tCD81-LEL, eE2 mutants

HVR1-eE2 (residues 406–656) and eE2 (full length, residues 384–656) from HCV genotype J6, and CD81 (residues 112-202 from human and tamarin) were expressed in HEK293T GnTI⁻ cells (Davide Comoletti, Rutgers University) and purified as described previously[31]. Briefly, the proteins of interest were cloned into a lentiviral vector containing an CMV promoter, a prolactin signal sequence, desired gene fragment, HRV3C cleavage site followed by a C-terminal protein-A and FLAG tags. Stable expressing GnTI⁻ HEK293T cells were produced by lentiviral transduction. Cells were grown in an adherent cell bioreactor (Cesco Bioengineering) for long-term growth and protein production. Supernatants were harvested every two days and purified by IgG affinity chromatography and eluted by GST-HRV3C protease digestion. The elution was purified by subtractive chromatography over GST and Q columns followed by size exclusion chromatography. Final yields for all constructs were 5-10 mg per liter of supernatant. eE2 mutants I422A, Y529A, W531A, and Y529A/W531A (double mutant) of eE2 (full length, residues 384–656) from HCV genotype J6 were cloned into the same plasmid and expressed in suspension Expi239 GnTI⁻ cell culture (ThermoFisher) by transient transfection method. An ExpiFectamine 293 transfection kit (ThermoFisher) was used per the manufacturer's protocol for high protein yield. Supernatants were harvested on the 6th day of post-transfection. eE2 mutants were purified by IgG, GST and Q column as detailed above.

Production, purification, and production of 2A12 Fab

The protocol is adapted from [12] with slight modification. The large-scale growth of the mouse 2A12 hybridoma (Arash Grakoui, Emory University School of Medicine) was achieved through CELLine Classic bioreactor flask (Sigma-Aldrich). 6×10^6 cells in 6 ml of IMDM media with 15% low-IgG FBS, and 10 mM HEPES pH 7.5 (culture media) were inoculated in the inner layer the cell, and upper membrane was covered with 350 ml of IMDM media with 1% low-IgG FBS, and 10 mM HEPES pH 7.5 (nutrient media). Culture

media was harvested after 4-6 days when hybridoma cell confluency reaches to 6 x 10^8 cells. Media was centrifuged at 1000 rpm for 20 min, and supernatant was further purified. 2A12 was purified through protein G column and dialyzed in 10 mM EDTA, 20 mM sodium phosphate pH 7.0. Just before digestion with papain, cysteine-HCl was added to a final concentration of 20 mM and pH was adjusted to 7.0. Approximately 100 μl immobilized agar bead papain (ThermoFisher) was used for 20 mg of 2A12 antibody and incubated for 3 hours at 37°C by gentle inversion. Reducing and non-reducing gels confirmed complete digestion of 2A12 antibody. Immobilized papain was separated by centrifuge at 4200 g at 4°C for 20 min. Supernatant was loaded on protein A column and flow through was collected and further loaded onto Protein G column which was pre-equilibrated with 20 mM HEPES pH7.5, 250 mM NaCl and 5% glycerol. 2A12 Fabs were eluted from Protein G column by 0.05% TFA, and immediately neutralize by 1 M Tris pH 8.0 and desalted into 20 mM Tris pH 8.0.

Crystallization

eE2/2A12 complex—2A12 Fab was incubated with eE2 at a ratio of 1.1:1 (w/w) for 1-2 hours at 4°C before purification over Superdex200 size exclusion column (Cytiva life sciences) equilibrated with 20 mM HEPES pH 7.5 and 100 mM NaCl. The complex was concentrated to 10mg/ml and crystals were grown at 4°C via hanging drop vapor diffusion method. 2μl of protein complex was mixed with 2μl of well solution containing 4% v/v tacsimate pH 5.0, 14% w/v PEG3350, and 4% D-(+)-trehalose dihydrate. Crystals were first seen after 7-8 days and continued to grow until day 10. Crystals were cryoprotected using well solution supplemented with 30% glycerol and flash cooled in liquid nitrogen. Data were collected at a wavelength of 0.979 Å using the Lilly Research Laboratories Collaborative Access Team (LRL-CAT) 31-ID beamline at the Advanced Photon Source (APS), Argonne National Laboratory.

Tamarin CD81-LEL—Tamarin CD81-LEL was purified over Superdex200 column equilibrated with 20 mM HEPES pH 7.5 and 100 mM NaCl. The protein was then concentrated to approximately 14 mg/ml before being grown into crystals using the hanging drop vapor diffusion method at 20°C. 2 μl of protein was mixed with equal amount of reservoir solution containing 0.1 M HEPES pH 7.5, and 55% PEG200. Single cubic crystals were obtained one day after setting up. Crystals were flash cooled in liquid nitrogen without additional cryoprotectant and data was collected at a wavelength of 0.979Å at Southeast Regional Collaborative Access Team (SER-CAT) 22-ID beamline at the APS, Argonne National Laboratory.

HVR1-eE2/2A12 Fab/tCD81-LEL—Initial crystallization trial with several different E2 and CD81-LEL constructs produced crystals that diffracted poorly (4.5Å resolution or worse). In an attempt to improve the resolution, plasmid encoded amino acids and HVR1 were removed from tCD81-LEL and eE2, respectively. HVR1-eE2 and 2A12 Fab complex was mixed in 1:1.2 w/w ratio and then mixed with tCD81-LEL in 1:1.2 molar ratio in a buffer containing 20 mM sodium acetate pH 4.5, 100 mM NaCl and incubated overnight on ice at 4°C. The complex was purified over a superdex200 column equilibrated with 20 mM sodium acetate pH 4.5, 100 mM NaCl. The complex was concentrated to 10 mg/ml

and crystals were grown at 4°C via hanging drop vapor diffusion method. Diffraction quality crystals were grown by microseeding in 0.2 M sodium acetate pH 4.5, 4% v/v tacsimate pH 4.0, 12% v/v PEG Smear Medium in 1 to 2 days after setting up 24-well plate. Crystals were cryoprotected in a stepwise manner with mother liquor supplemented with 30% v/v PEG Smear Medium, and flash cooled in liquid nitrogen. Data were collected at 0.979 Å at SER-CAT 22-ID beamline at the APS, Argonne National Laboratory. SER-CAT is supported by its member institutions, and equipment grants (S10_RR25528 and S10_RR028976) from the National Institutes of Health.

Structure determination and refinement

eE2 (genotype J6) –2A12Fab crystals belong to space group *C222₁* with cell parameters a=95.84Å, b=155.56Å, c=129.42Å. Phases were determined by the molecular replacement method using PHENIX_phaser[32] and the coordinates were obtained from PDB entry 4WEB. Unambiguous placement of the Fab heavy and light chains provided the necessary phases to extend the map to cover eE2 coordinates, using iterative rounds of model building and density modification by COOT[33], and the model was evaluated during refinement for various parameters. The final model was built to a resolution of 2.71 Å, comprising residues 422–523, 490–571, and 596–650 of eE2 from the J6 genome with six *N*-linked, *N*-acetylglucosamine, one BMA[34], and 102 solvents molecules. 2A12 Fab light chain and heavy chain is consist of 1–218 and 1-219 amino acids, respectively. The model coordinates were refined to R_{work} 0.218 and R_{free} 0.271 with 92.11% Ramachandran favored, allowed 7.05, and 0.84% outliers calculated from MolProbity[35]. The overall $CC_{1/2}$ of the processed data is 0.989 while $CC_{1/2}$ in the outer shell is 0.487.

Tamarin CD81-LEL crystals belong to space group *I23* with cell parameters a=113.26Å, b=113.26Å, c=113.26Å, and data were collected at 1.80Å resolution. PDB entry 5TCX was truncated to LEL and the chain was mutated to polyalanine. The edited model was used to determine the initial phases by using PHENIX_phaser[32]. Iterative rounds of model building in COOT[33] and refinement in PHENIX_refine led the R_{work} 0.207 and R_{free} 0.231 with 96.83% Ramachandran favored, 3.17% allowed, and 0% outliers. Chain A and chain B start from 106-201 and 106-202, respectively. Residues 106-111 were from the backbone of pJG construct which were also built in the electron density with 66 solvent, two polyethylene glycol, and one glycerol molecule. The overall $CC_{1/2}$ of the processed data is 0.997 while outer shell $CC_{1/2}$ is 0.612.

HVR1-eE2/2A12 Fab/tCD81-LEL complex crystals belong to space group *P2₁2₁2₁* with cell parameters a=76.95Å, b=127.77Å, c=212.37Å. Phases were determined by the molecular replacement method using PHENIX_phaser[32] and the Fab coordinates were taken from eE2 J6-2A12Fab structure. We found two molecules per asymmetric unit, and further HVR1-eE2 and tCD81 coordinate were placed by PHENIX_phaser which further improved the phases. The model was built and refined in COOT[33] and refined in PHENIX_refine at 3.32Å resolution. The final structure was comprised of chain C 418–453, 490–571 and 597–650 residues, and chain G 415–453, 490–571, and 596–654 from the of HVR1-eE2. Both heavy chains (A, E) and light chains (B, F) of 2A12 Fab consist of 1-218 amino acids. Chains D and H of tamarin CD81 consist of 119-199 and 116-199 residues,

respectively. Seven *N*-linked *N*-acetylglucosamine and one BMA were also modeled in the structure[34] with refined R_{work} 0.241 and R_{free} 0.286, and 91.87% Ramachandran favored, 7.4% allowed and 0.73% outliers. The overall $CC_{1/2}$ of the processed data is 0.994 while $CC_{1/2}$ in the outer shell is 0.398. The statistics of all three data processing and structure refinement are summarized in Extended Data Table 2.

Sequence alignment and surface electrostatic potential

Multiple sequence alignment was performed by Clustal Omega[36]. While surface electrostatic potential was visualized via Pymol with the assistance of APBS[37] plugin. The input files for APBS plugin at different pH 5.0 and 7.5 were generated from the online APBS server (http://apbs.poissonboltzmann.org/) using PDB2PQR tools[38] using the default setting for forcefield and output naming scheme. All structural figures were prepared by PyMol[39].

Isothermal Titration Calorimetry and Data Analysis

The protein samples were dialyzed against buffers containing 20 mM HEPES pH 7.5 and 100 mM NaCl, or 20 mM Sodium citrate pH 5.0 and 100 mM NaCl. A MicroCal ITC-200 isothermal calorimeter was used to carry out calorimetric experiments at 20°C with stirring at 750 rpm (Malvern Panalytical, UK). The interface between the cell, containing 15-30 μM eE2, and the syringe was equilibrated with 0.4 μL (0.14–0.19 μM tCD81-LEL and 0.30–0.58 μM hCD81-LEL) of ligand with a spacing of 0.8 seconds, followed by 16 subsequent injections of 2.45 μL (0.87–1.17 μM tCD81-LEL and 1.82–3.51 μM hCD81-LEL) with a spacing of 180 seconds.

ITC thermograms were integrated using the NITPIC program[40] and normalized peak area plots were fitted using SEDPHAT[41]. The A + B $\rightleftarrows$ AB heterodimer model was used to determine eE2-CD81 interaction. Enthalpogram fitting parameters included K_D and ΔH while eE2 was considered the incompetent fraction. Binding parameter confidence level of 95% and error surface of the fit were estimated with SEDPHAT. ITC measurements were performed at the NHLBI Biophysics Core Facility.

Liposome flotation assay

3 μg of wild-type or mutant eE2 was mixed with 3.6 μg tCD81-LEL (a 6-fold excess of tCD81-LEL) or buffer. The volume was adjusted to 50 μl with either 20 mM sodium citrate pH 5.0, 100 mM NaCl or 20 mM HEPES pH 7.5, 100 mM NaCl buffer. The sample was incubated on ice overnight at 4°C. 50 μl of 200 nm Soy PC: Cholesterol liposomes (70:30 molar ratio) from Encapsula NanoSciences LLC (stock 10 mM or 8 μg/μl) (cat no CPC-610) were added and incubated at 37°C for 1 hour. After incubation, 67 μl of 3 M KCl was added to a final concentration of 1 M KCl and incubated at 37°C for 15 min to minimize the nonspecific electrostatic association between proteins and lipids. Then 67% (w/v) sucrose in matching buffer was added to a final concentration of 40% in a final volume of 500 μl, mixed thoroughly, and underlaid in a buffer-matched, step gradient of 0.5 ml 5% and 10 ml of 25% (w/v) sucrose in an Open-Top Thinwall Ultra-Clear Centrifuge Tube (Beckman Coulter, 344060). Gradients were centrifuged at 281,000 x g for 75 min at 4°C in an SW 40 Ti swinging bucket rotor (Beckman Coulter Optima XL-100K Ultracentrifuge). After

centrifugation, each gradient was fractionated, from the top down, into 16 fractions of 700 μl. Samples were analyzed by Western blot.

Western blot analysis

All the fractions were diluted with 10x SDS-PAGE reducing sample buffer to a final concentration of 1x and denatured at 95°C for 5 min. Samples were run either along with eE2FL marker (std) and Odyssey Protein Molecular Weight Marker (Li-Cor) (L) on 4-20% Bis-Tris precast gels (Bio-Rad). Proteins were then transferred to PVDF membranes using a Trans-Blot Turbo Transfer System (Bio-Rad). The membrane was blocked by Intercept (PBS) Blocking Buffer (LI-COR) for 1 hour at 37°C followed by incubating the blot with a 1:1000 dilution of purified 2C1 mouse antibody (against HVR1 of HCV J6 E2 produced in Dr. Arash Grakoui's laboratory) and incubated overnight at 4°C. Primary antibody dilution was prepared in Odyssey Blocking Buffer in PBS with 0.1% Tween 20 (Sigma-Aldrich). The secondary antibody, IRDye 800CW Goat anti-Mouse IgG (Li-Cor), was used in 1:10,000 dilution. The Western blot was scanned using Li-Cor Odyssey software (version 3.0). Fluorescence signals of top fractions were background corrected and measured by the Image Studio Lite software (version 5.2.5). The fluorescence intensities were exported in excel format and histograms were prepared.

Extended Data

A

```
Human    MGVEGCTKCIKYLLFVFNFVFWLAGGVILGVALWLRHDPQTTNLLYLELGDKPAPNTFYVGIYILIAVGAVMMF
Tamarin  MGVEGCTKCIKYLLFVFNFVFWLAGGVILGVALWLRHDPQTTNLLYLELGDKPAPNTFYVGIYILIAVGAVMMF


Human    VGFLGCYGAIQESQCLLGTFFTCLVILFACEVAAGIWGFVNKDQIAKDVKQFYDQALQQAVVDDDANNAKAVVK
Tamarin  VGFLGCYGAIQESQCLLGTFFTCLVILFACEVAAGIWGFVNKDQIAKDVKQFYDQALQQAVVDDDANNAKAVVK


Human    TFHETLDCCGSSTLTALTTSVLKNNLCPSGSNIISNLFKEDCHQKIDDLFSGKLYLIGIAAIVVAVIMIFEMI
Tamarin  TFHETLNCCGSSTLSALTTSMLKNNLCPSGSSIISNLFKEDCHQKIDELFSGKLYLIGIAAIVVAVIMIFEMI


Human    LSMVLCCGIRNSSVYVP
Tamarin  LSMVLCCGIRNSSVY--
```

B
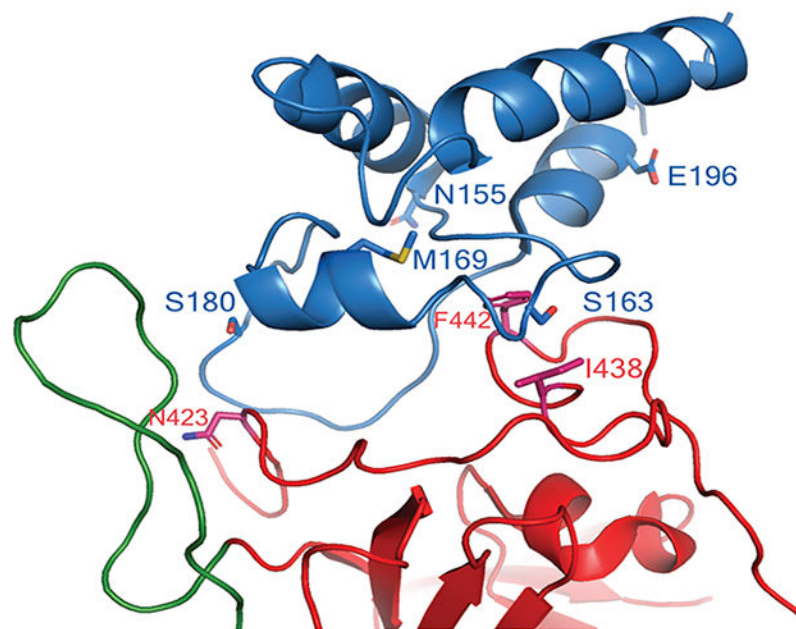
Extended Data Figure 1. Sequence divergence between human and tamarin CD81.
(A) Sequence alignment (light blue and black font) of full-length human and tamarin CD81 (Accession numbers: Human NM_004356, Tamarin CAB89875.1). The CD81-LEL (black font) has five divergent residues (green and yellow highlights represent nonidentical and similar amino acids, respectively). (B) Ribbon diagram of tamarin CD81-LEL (blue) bound to HVR1-eE2 (red and CD81-binding loop green) with side chains of the five, diverging CD81 residues (blue sticks) and proximal residues in eE2 (red sticks).
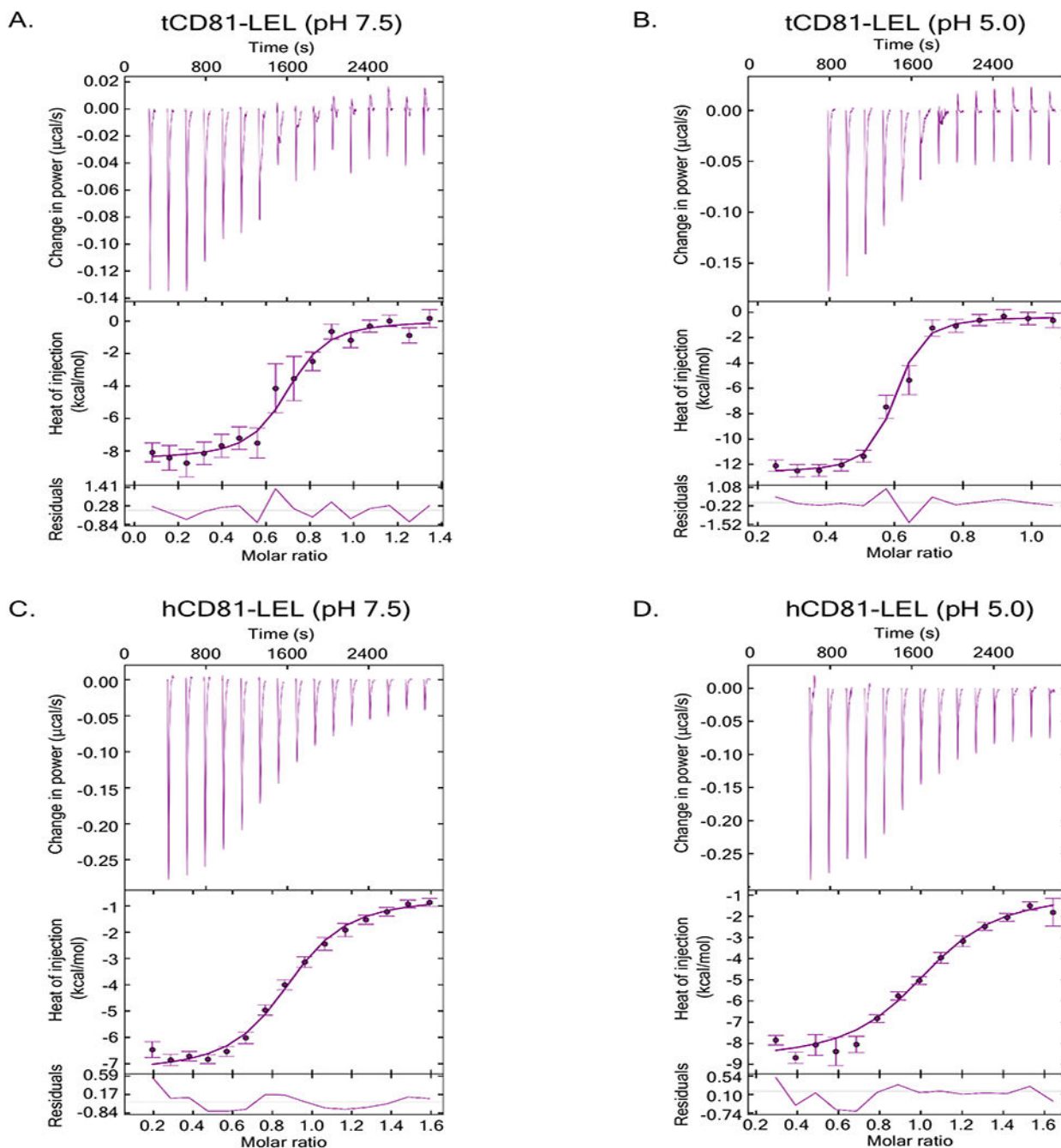
Extended Data Figure 2. Thermodynamic characterization of tamarin and human CD81-LEL interaction with eE2.

ITC for the titration of tCD81-LEL (A and B) or hCD81-LEL (C and D) into eE2 at pH 7.5 (A and C) and pH 5.0 (B and D). Thermogram (upper panel), integrated heats and error bars (middle panel), and fit residuals (lower panel) are shown for each. The measurements were performed at 20° C and analyzed with an A + B ⇌ AB heterodimer model. Error bars indicate the error of peak integration over an interpolated baseline with a 68% (1 sigma) confidence interval. Residuals are the Y-axis difference between the data point and the fitted curve in kcal/mol.
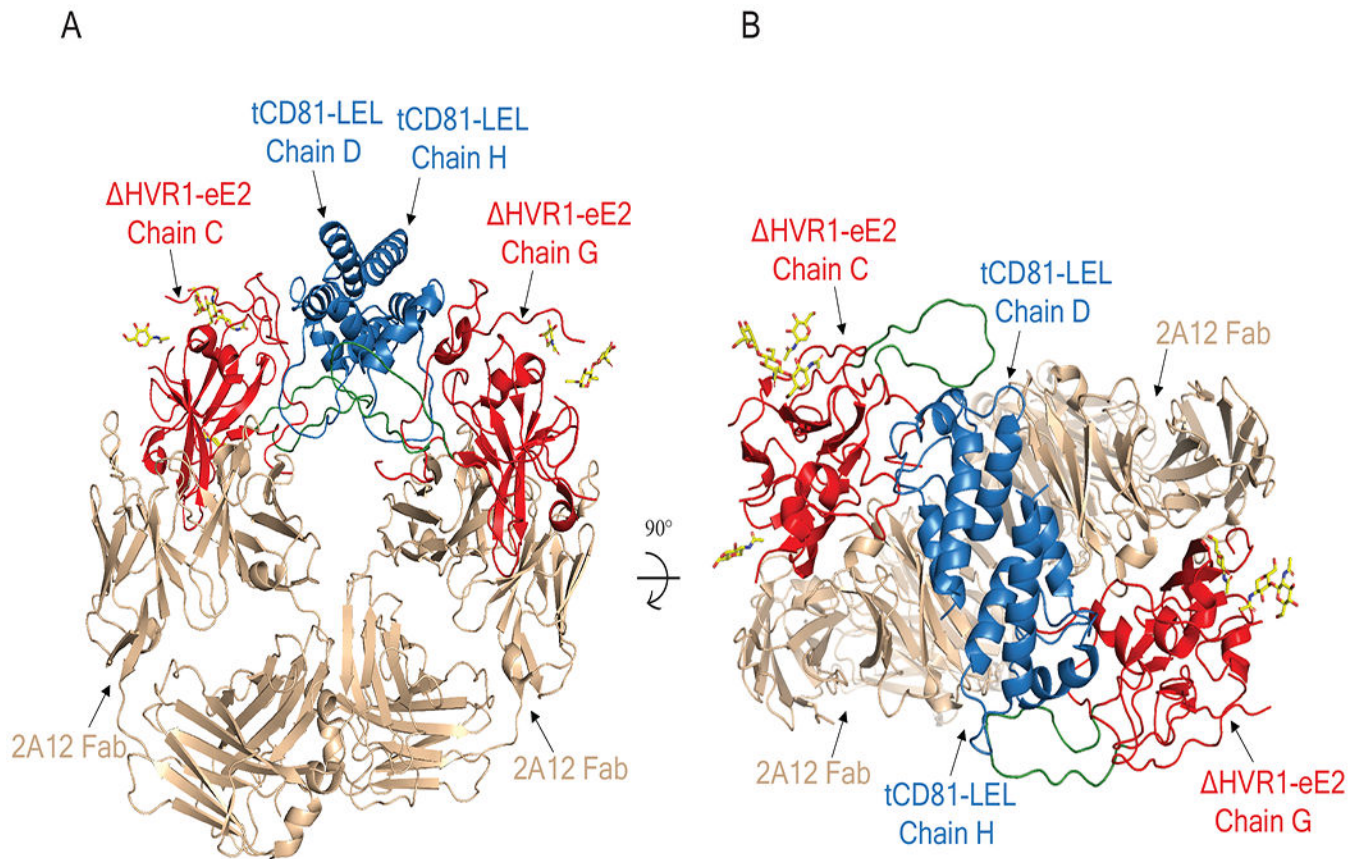
Extended Data Figure 3. The asymmetric unit for the tCD81-LEL/ HVR1-eE2/2A12 complex.
HVR1-eE2 chains C and G (red with extended CD81-binding loop in green), tCD81-LEL
chains D and H (blue), 2A12 (wheat) ribbon diagrams in the asymmetric unit of the tCD81-
LEL/ HVR1-eE2/2A12 complex from side (left) and top (right) views. The 90° axis of
rotation is indicated. Carbohydrate moieties (yellow heteroatom sticks) are also shown.

A

B

Extended Data Figure 4. Diagram and conservation of HCV E2.

(A) Schematic representation of the E2 protein with the CD81-binding loop highlighted in yellow and the asterisks highlighting regions associated with CD81 binding. (B) Multiple sequence alignment of eE2 from representative strains (as labeled) of the seven genotypes. Conserved residues (cyan highlights) and CD81-binding loop residues (red font) are noted. Asterisks indicate residues 4Å from tCD81 common to both chains C and G (red), chain G only (blue), and chain A only (green). Hypervariable region, antigenic site, and transmembrane are labeled HVR, AS, and TM, respectively.
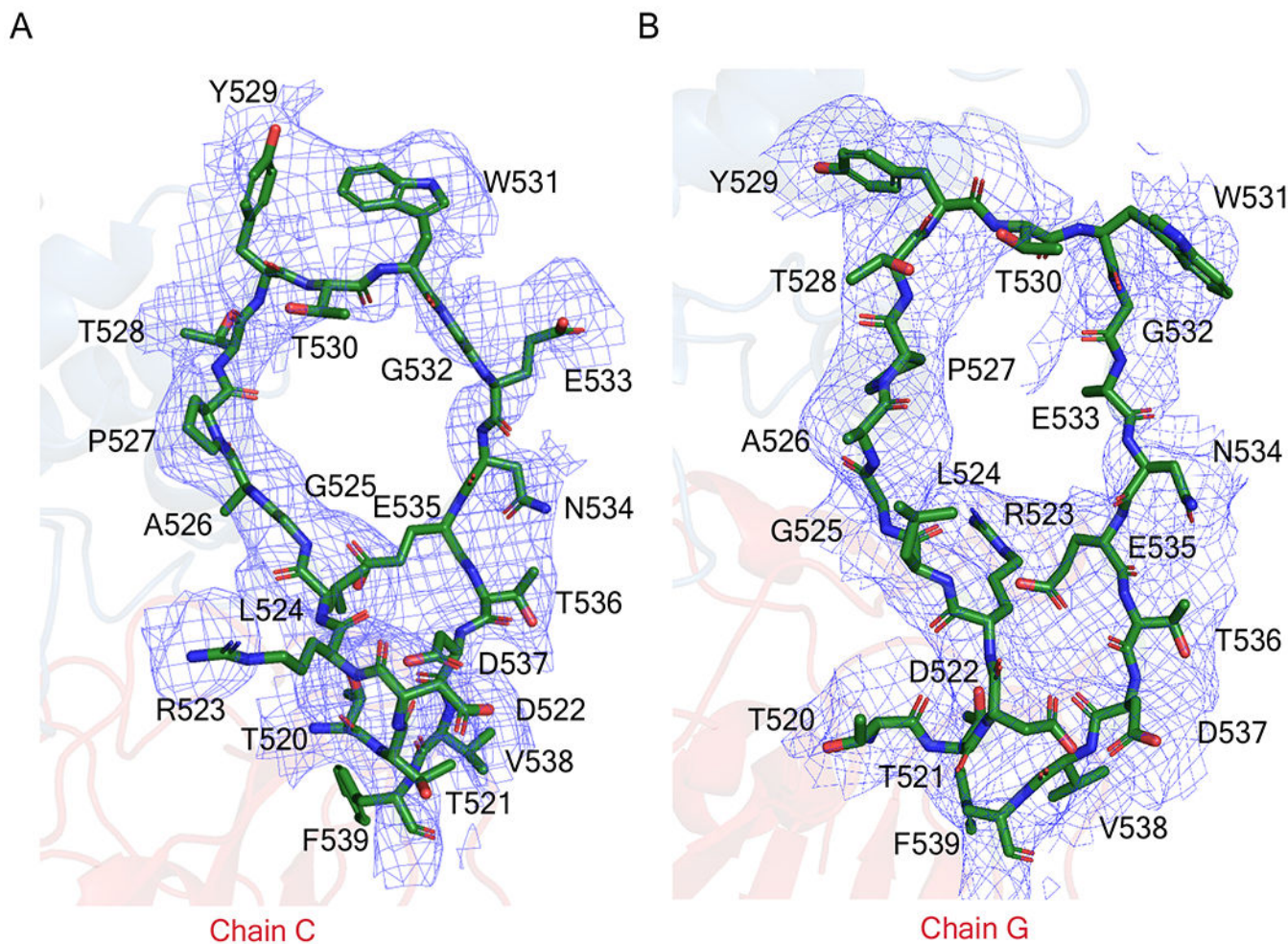
Extended Data Figure 5. A simulated-annealing *2F$_O$-F$_C$* composite omit map for the HVR1-eE2 CD81-binding loop in the X-ray crystal structure of the complex.
CD81-binding loop in (A) Chain C and (B) Chain G (green heteroatom sticks), residues as labeled, in a 0.8σ contour level *2F$_O$-F$_C$* composite omit map (blue mesh) calculated from the omission of residues 415–426 and 520–539, and packed against the tCD81-LEL (blue) and HVR1-eE2 (red) ribbon diagrams.

A
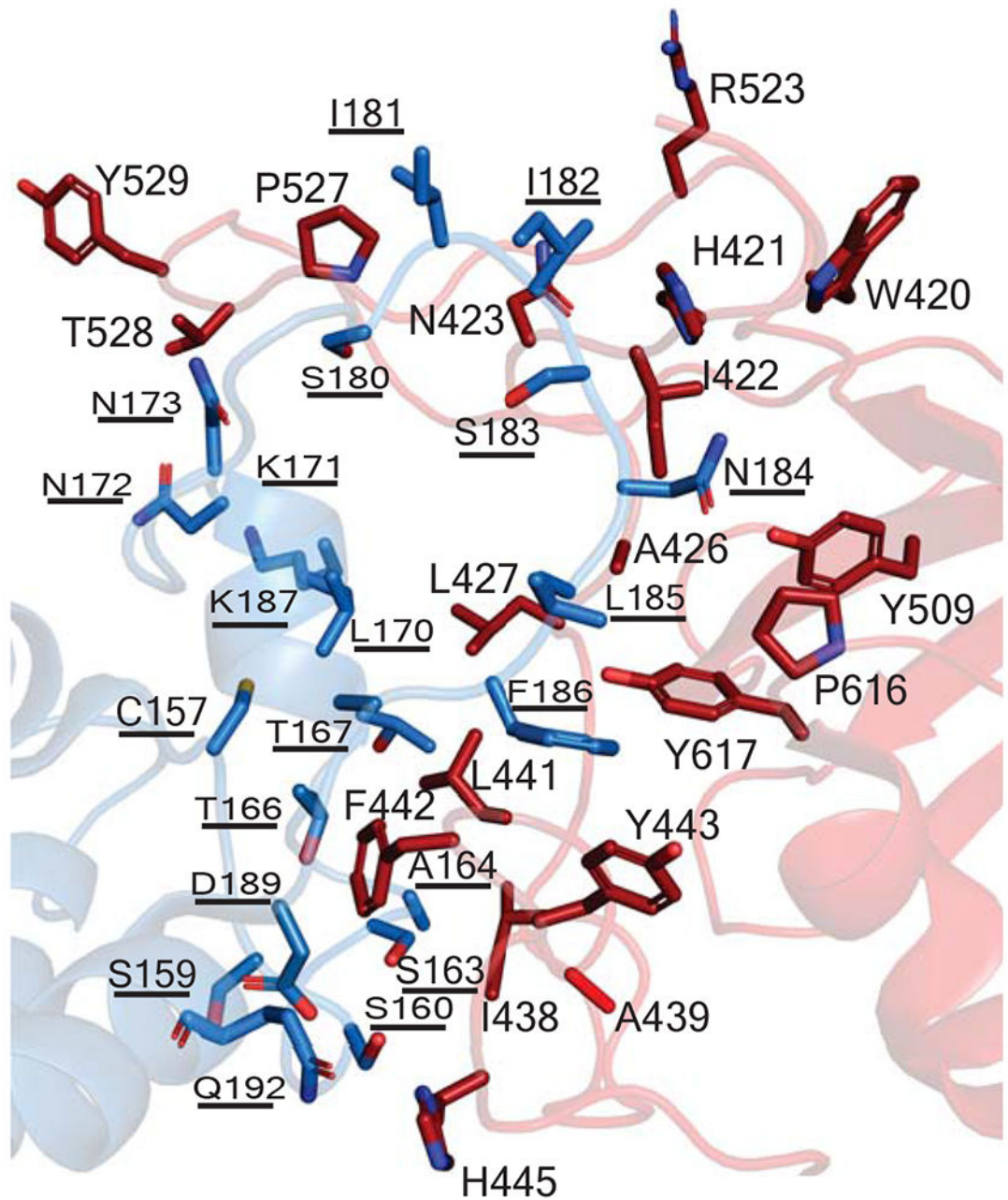
Extended Data Figure 6. Interface between tCD81-LEL and HVR1-eE2.
Ribbon diagram of tCD81-LEL (blue) and HVR1-eE2 (red) interface, chains C and D, with side chains (blue and red heteroatom sticks, respectively). The labels for tCD81-LEL residues are underlined.
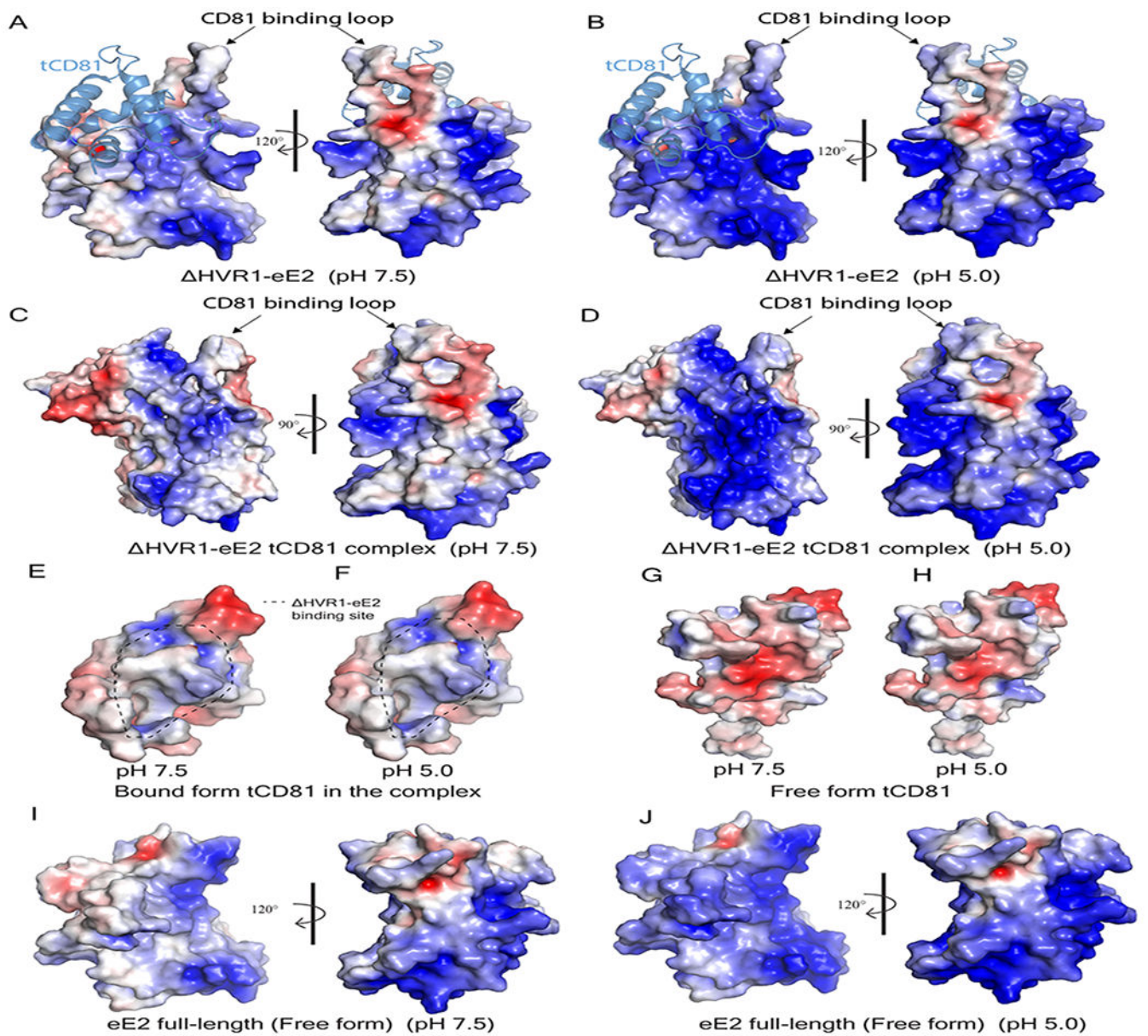
Extended Data Figure 7. Electrostatic-potential surface maps of E2 and tCD81-LEL.
Electrostatic-potential surface maps of ΔHVR1-eE2 in complex (A and B), tCD81-LEL/ΔHVR1-eE2 complex (C and D), tCD81-LEL in complex (E and F) and free form (G and H), and full-length eE2 free form (I and J). The surfaces are colored by electrostatic potential corresponding to +5 kcal/(mol·e) (blue) and −5 kcal/(mol·e) (red) at 298 K calculated at pH 7.5 (A, C, E, G, and I) and 5.0 (B, D, F, H, and J) as labeled. Panels A, B, I, and J are depicted in the same orientation; panels E–H are depicted in the same orientation. (A and B) tCD81-LEL is shown as a transparent, blue ribbon diagram. (E and F) The ΔHVR1-eE2 binding surface is outlined with a dotted line.
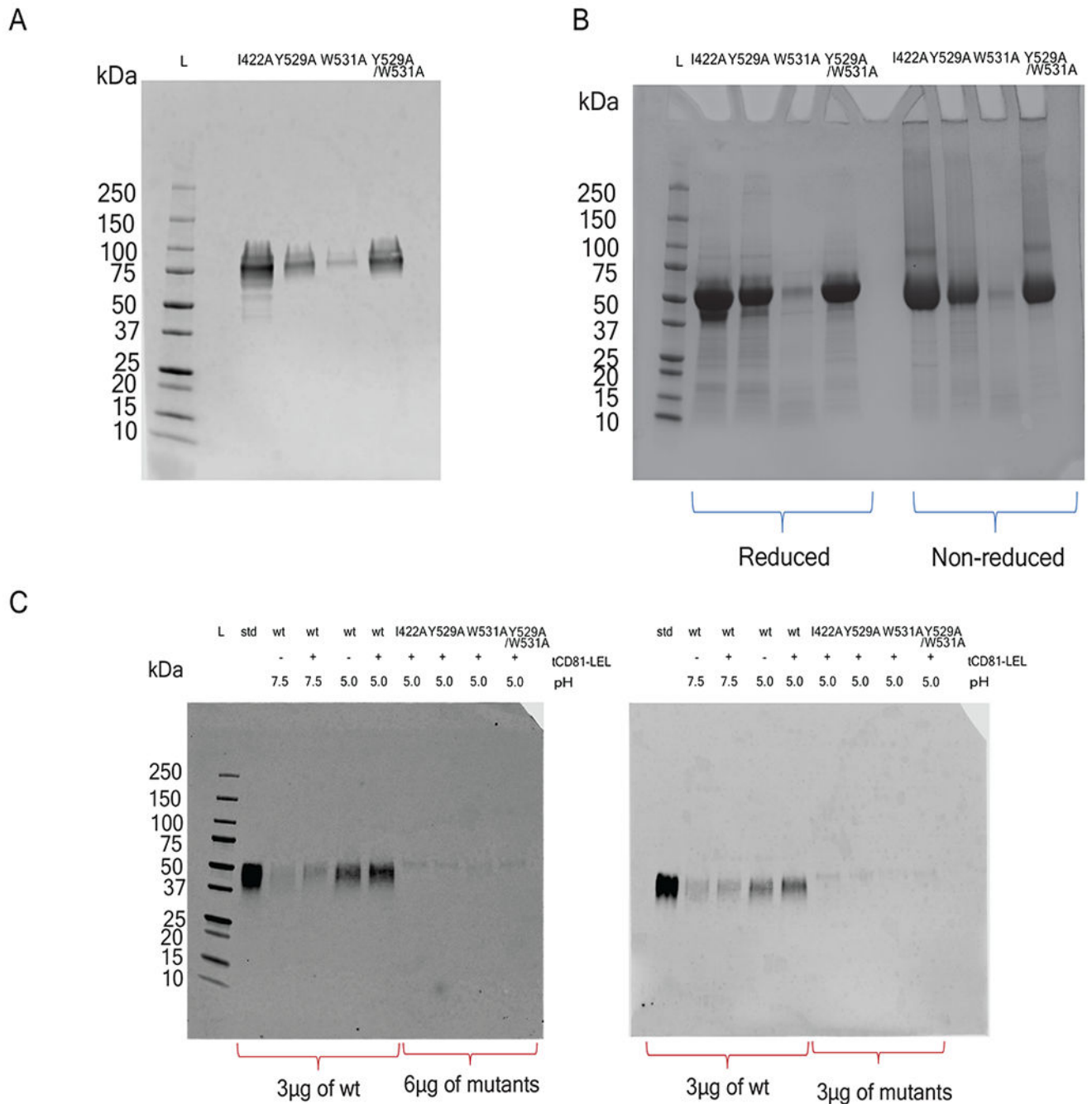
Extended Data Figure 8. Expression, purification, and liposome floatation of eE2 mutants
(A) E2-specific Western blot of cell culture supernatants showing secreted protein levels of eE2 mutants I422A, Y529A, W531A, and double mutant Y529A/W531A. Expi293 GnTI- cells were transfected and supernatants (uncleaved eE2 protein) were mixed with reduced 2x sample buffer. 15 ul of supernatant was loaded in each well. E2 2C1 primary antibody was used for western blotting. (B) Coomassie-stained 4-20% Bis-Tris SDS-PAGE gels of purified eE2 mutant proteins in the presence (Reduced) and absence (Non-reduced) of β-mercaptoethanol. (C) E2-specific Western blot of top fractions from liposome flotation

assays, comparing increased loading (as labeled under each blot) of mutants. Protein molecular weight maker (L) and wild-type eE2 is provided as a marker (std). Sample pH, inclusion of tCD81-LEL, and eE2 mutant proteins are labeled. (D) Gel source data for Figure 4C.

Extended Data Table 1
Affinity measurements of eE2 to human and tamarin CD81-LEL at neutral and low pH.

Numbers in parentheses represent 95% confidence intervals.

Substrate	Ligand	pH	H (kcal/mol)	K_d (nM)	N
	tCD81	7.5	−8.52 (−11.21, −6.98)	175 (14, 870)	0.67 (0.57, 0.76)
eE2	tCD81	5.0	−12.27 (−13.67, −11.12)	37 (8, 100)	0.57 (0.54, 0.61)
	hCD81	7.5	−6.65 (−8.09, −5.76)	773 (316, 1905)	0.86 (0.81, 0.94)
	hCD81	5.0	−7.89 (−10.10, −6.09)	681 (208, 1698)	0.99 (0.89, 1.31)

Extended Data Table 2
Data collection and refinement statistics for eE2/2A12, tCD81-LEL and tCD81-LEL/ HVR1-eE2/2A12 complex.

*Single crystal was used for each data collection. *Values in parentheses are for highest-resolution shell.

	eE2/2A12	tCD81-LEL	tCD81-LEL/ HVR1-eE2/2A12
Data collection			
Space group	$C222_1$	I23	$P2_12_12_1$
Cell dimensions *a, b, c* (Å)	95.84, 155.56, 129.42	113.26, 113.26, 113.26	76.95, 127.77, 212.37
(°)	90, 90, 90	90, 90, 90	90, 90, 90
Resolution (Å)	33.34-2.71(2.81-2.71)	46.24-1.80 (1.83-1.80)	54.74-3.32 (3.5-3.32)
R_{sym}	0.11 (0.49)	0.18 (3.74)	0.28 (6.4)
$I / \sigma I$	6.3 (2.0)	14.2 (1.7)	6.8 (1.2)
Completeness (%)	99.01 (98.48)	100 (100)	99.5 (100)
Redundancy	1.98 (1.95)	40.1 (41.4)	13.2 (13.2)
Refinement Resolution (Å)	33.34-2.71 (2.81-2.71)	40.04-1.80 (1.87-1.79)	52.10-3.32 (3.4-3.32)
No. reflections	26376 (2583)	22508 (2237)	31547 (3090)
R_{work} / R_{free}	0.2183/0.2705	0.2072/0.2309	0.2413/0.2856
No. atoms			
Protein	606	193	1389
Ligand/ion	95	32	109
Water	102	66	0
B-factors			
Protein	56.48	57.59	167.40
Ligand/ion	127.91	82.34	252.70
Water	34.0	60.86	0

	eE2/2A12	tCD81-LEL	tCD81-LEL/ HVR1-eE2/2A12
R.m.s. deviations			
Bond lengths (Å)	0.005	0.014	0.002
Bond angles (°)	0.847	1.379	0.668
Ramachandran plot (%)			
Favored	92.11	96.83	91.87
Allowed	7.05	3.17	7.4
Outliers	0.84	0	0.73

Extended Data Table 3

Residues making interactions within 4Å

Amino acids in bold letters represent the CD81-binding loop, and those in red represent shared interactions in the both chains of HVR1-eE2.

	HVR1-eE2 chain C	tCD81-LEL chain D
1	TRP 420	ASN 184
2	TRP 420	PHE 186
3	HIS 421	SER 183
4	ILE 422	SER 183
5	ILE 422	ILE 182
6	ASN 423	ILE 181
7	LEU 427	THR 167
8	LEU 441	THR 166
9	PHE 442	SER 159
10	PHE 442	SER 163
11	PHE 442	THR 166
12	PHE 442	CYS 157
13	PHE 442	PHE 186
14	PHE 442	LYS 187
15	TYR 443	PHE 186
16	HIS 445	SER 160
17	HIS 445	GLN 192
18	TYR 509	ASN 184
19	**THR 528**	**ASN 172**
20	**THR 528**	**ASN 173**
21	PRO 616	ASN 184
22	TYR 617	LEU 185
23	TYR 617	PHE 186

	HVR1-eE2 chain G	tCD81-LEL chain H
1	ASN 415	SER 180

	HVR1-eE2 chain G	tCD81-LEL chain H
2	ASN 415	ILE 181
3	THR 416	SER 180
4	ALA 426	LYS 171
5	ASN 428	THR 167
6	ILE 438	SER 163
7	ILE 438	ALA 164
8	ALA 439	SER 163
9	LEU 441	PHE 186
10	PHE 442	THR 166
11	PHE 442	LEU 170
12	TYR 443	SER 160
13	TYR 443	ASP 189
14	HIS 445	SER 160
15	**ARG 523**	**LYS 171**
16	**PRO 527**	**LYS 171**
17	**PRO 527**	**ASN 172**
18	**TYR 529**	**ASN 172**
19	TYR 617	LEU 185
20	TYR 617	PHE 186
21	TYR 617	ASN 184

Supplementary Material

Refer to Web version on PubMed Central for supplementary material.

Acknowledgements

Data availability

The coordinates and structure factors for eE2/2A12, tCD81-LEL and tCD81-LEL/DHVR1-eE2/2A12 have been deposited into the RCSB Protein Data Bank (https://www.rcsb.org) under accession numbers 7MWW, 7MWS and 7MWX, respectively.

Main references

1. Gerold G, Moeller R & Pietschmann T Hepatitis C Virus Entry: Protein Interactions and Fusion Determinants Governing Productive Hepatocyte Invasion. Cold Spring Harb Perspect Med 10, (2020).

2. Tzarum N, Wilson IA & Law M The Neutralizing Face of Hepatitis C Virus E2 Envelope Glycoprotein. Front Immunol 9, 1315, (2018). [PubMed: 29951061]

3. Tscherne DM et al. Time- and temperature-dependent activation of hepatitis C virus for low-pH-triggered entry. J Virol 80, 1734–1741, (2006). [PubMed: 16439530]

4. Rothwangl KB, Manicassamy B, Uprichard SL & Rong L Dissecting the role of putative CD81 binding regions of E2 in mediating HCV entry: putative CD81 binding region 1 is not involved in CD81 binding. Virology Journal 2008 5:46 5, 46, (2008).

5. Drummer HE, Wilson KA & Poumbourios P Identification of the hepatitis C virus E2 glycoprotein binding site on the large extracellular loop of CD81. J Virol 76, 11143–11147 (2002). [PubMed: 12368358]

6. Drummer HE, Boo I, Maerz AL & Poumbourios P A conserved Gly436-Trp-Leu-Ala-Gly-Leu-Phe-Tyr motif in hepatitis C virus glycoprotein E2 is a determinant of CD81 binding and viral entry. J Virol 80, 7844–7853, (2006). [PubMed: 16873241]

7. Owsianka AM et al. Identification of conserved residues in the E2 envelope glycoprotein of the hepatitis C virus that are critical for CD81 binding. J Virol 80, 8695–8704, (2006). [PubMed: 16912317]

8. Zhao Z et al. A neutralization epitope in the hepatitis C virus E2 glycoprotein interacts with host entry factor CD81. PLoS One 9, e84346, (2014). [PubMed: 24400084]

9. Higginbottom A et al. Identification of amino acid residues in CD81 critical for interaction with hepatitis C virus envelope glycoprotein E2. J Virol 74, 3642–3649 (2000). [PubMed: 10729140]

10. Flint M et al. Diverse CD81 proteins support hepatitis C virus infection. J Virol 80, 11331–11342, (2006). [PubMed: 16943299]

11. Allander T, Forns X, Emerson SU, Purcell RH & Bukh J Hepatitis C virus envelope protein E2 binds to CD81 of tamarins. Virology 277, 358–367, (2000). [PubMed: 11080483]

12. Khan AG et al. Structure of the core ectodomain of the hepatitis C virus envelope glycoprotein 2. Nature 509, 381–384, (2014). [PubMed: 24553139]

13. Kitadokoro K et al. CD81 extracellular domain 3D structure: insight into the tetraspanin superfamily structural motifs. EMBO J 20, 12–18, (2001). [PubMed: 11226150]

14. Cunha ES et al. Mechanism of Structural Tuning of the Hepatitis C Virus Human Cellular Receptor CD81 Large Extracellular Loop. Structure 25, 53–65, (2017). [PubMed: 27916518]

15. Dearborn AD & Marcotrigiano J Hepatitis C Virus Structure: Defined by What It Is Not. Cold Spring Harb Perspect Med 10, (2020).

16. Susa KJ, Rawson S, Kruse AC & Blacklow SC Cryo-EM structure of the B cell co-receptor CD19 bound to the tetraspanin CD81. Science 371, 300–305, (2021). [PubMed: 33446559]

17. Flyak AI et al. HCV Broadly Neutralizing Antibodies Use a CDRH3 Disulfide Motif to Recognize an E2 Glycoprotein Site that Can Be Targeted for Vaccine Design. Cell Host Microbe 24, 703–716 e703, (2018). [PubMed: 30439340]

18. Kong L et al. Hepatitis C virus E2 envelope glycoprotein core structure. Science 342, 1090–1094, (2013). [PubMed: 24288331]

19. Flyak AI et al. An ultralong CDRH2 in HCV neutralizing antibody demonstrates structural plasticity of antibodies against E2 glycoprotein. Elife 9, (2020).

20. Tzarum N et al. Genetic and structural insights into broad neutralization of hepatitis C virus by human VH1-69 antibodies. Sci Adv 5, eaav1882, (2019). [PubMed: 30613781]

21. Zimmerman B et al. Crystal Structure of a Full-Length Human Tetraspanin Reveals a Cholesterol-Binding Pocket. Cell 167, 1041–1051 e1011, (2016). [PubMed: 27881302]

22. Rajesh S et al. Structural basis of ligand interactions of the large extracellular domain of tetraspanin CD81. J Virol 86, 9606–9616, (2012). [PubMed: 22740401]

23. Vasiliauskaite I et al. Conformational Flexibility in the Immunoglobulin-Like Domain of the Hepatitis C Virus Glycoprotein E2. mBio 8, (2017).

24. Lomize MA, Pogozheva ID, Joo H, Mosberg HI & Lomize AL OPM database and PPM web server: resources for positioning of proteins in membranes. Nucleic Acids Res 40, D370–376, (2012). [PubMed: 21890895]

25. Kielian M Mechanisms of Virus Membrane Fusion Proteins. Annu Rev Virol 1, 171–189, (2014). [PubMed: 26958720]

26. Boo I et al. Distinct roles in folding, CD81 receptor binding and viral entry for conserved histidine residues of hepatitis C virus glycoprotein E1 and E2. Biochem J 443, 85–94, (2012). [PubMed: 22240035]

27. Sharma NR et al. Hepatitis C virus is primed by CD81 protein for low pH-dependent fusion. J Biol Chem 286, 30361–30376, (2011). [PubMed: 21737455]

28. Owsianka AM et al. Identification of conserved residues in the E2 envelope glycoprotein of the hepatitis C virus that are critical for CD81 binding. J Virol 80, 8695–8704, (2006). [PubMed: 16912317]

29. White JM & Whittaker GR Fusion of Enveloped Viruses in Endosomes. Traffic 17, 593–614, (2016). [PubMed: 26935856]

30. Li HF, Huang CH, Ai LS, Chuang CK & Chen SS Mutagenesis of the fusion peptide-like domain of hepatitis C virus E1 glycoprotein: involvement in cell fusion and virus entry. J Biomed Sci 16, 89, (2009). [PubMed: 19778418]

Methods references

31. Yost SA, Whidby J, Khan AG, Wang Y & Marcotrigiano J Overcoming Challenges of Hepatitis C Virus Envelope Glycoprotein Production in Mammalian Cells. Methods Mol Biol 1911, 305–316, (2019). [PubMed: 30593635]

32. Adams PD et al. PHENIX: building new software for automated crystallographic structure determination. Acta crystallographica. Section D, Biological crystallography 58, 1948–1954 (2002). [PubMed: 12393927]

33. Emsley P & Cowtan K Coot: model-building tools for molecular graphics. Acta Crystallogr D Biol Crystallogr 60, 2126–2132 (2004). [PubMed: 15572765]

34. Emsley P & Crispin M Structural analysis of glycoproteins: building N-linked glycans with Coot. Acta Crystallogr D Struct Biol 74, 256–263, (2018). [PubMed: 29652253]

35. Chen VB et al. MolProbity: all-atom structure validation for macromolecular crystallography. Acta Crystallogr D Biol Crystallogr 66, 12–21, (2010). [PubMed: 20057044]

36. Madeira F et al. The EMBL-EBI search and sequence analysis tools APIs in 2019. Nucleic Acids Res 47, W636–W641, (2019). [PubMed: 30976793]

37. Baker NA, Sept D, Joseph S, Holst MJ & McCammon JA Electrostatics of nanosystems: application to microtubules and the ribosome. Proc Natl Acad Sci U S A 98, (2001).

38. Dolinsky TJ, Nielsen JE, McCammon JA & Baker NA PDB2PQR: an automated pipeline for the setup of Poisson-Boltzmann electrostatics calculations. Nucleic Acids Res 32, W665–667, doi:10.1093/nar/gkh381 (2004). [PubMed: 15215472]

39. DeLano WL The PyMOL molecular graphics system, <http://www.pymol.org> (2002).

40. Keller S et al. High-precision isothermal titration calorimetry with automated peak-shape analysis. Anal Chem 84, 5066–5073, (2012). [PubMed: 22530732]

41. Zhao H, Piszczek G & Schuck P SEDPHAT--a platform for global ITC analysis and global multi-method analysis of molecular interactions. Methods 76, 137–148, (2015). [PubMed: 25477226]
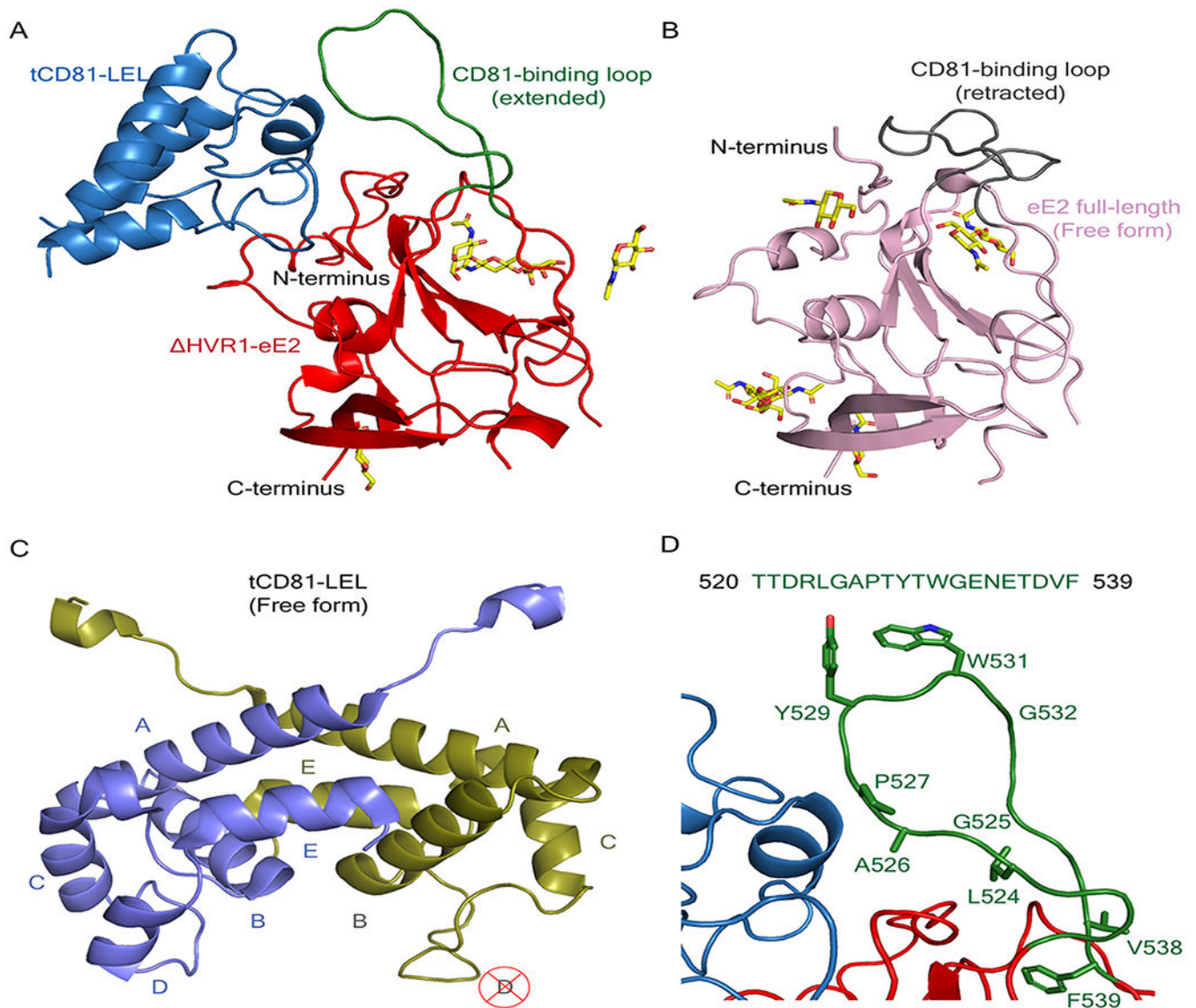
Figure 1: Ribbon diagrams of the tCD81-LEL/ HVR1-eE2/2A12, eE2/2A12, and tCD81-LEL X-ray crystal structures.

(A) tCD81-LEL(blue)/ HVR1-eE2(red/green) complex and (B) eE2 (pink/gray) alone, highlighting the location of the CD81-binding loop (green and gray, respectively). The 2A12 Fab is not shown. Carbohydrate molecules are colored by heteroatom. (C) The homodimeric, asymmetric unit of tCD81-LEL, free form, with helices A–E labeled on the intermediate (violet) and open (olive) conformations. The unwound helix D in the open conformation is labeled with a crossed-out D. (D) tCD81-LEL(blue)/ HVR1-eE2(red/green) interface in detail with the side chains of the CD81-binding loop residues (green and heteroatom) represented in sticks. The CD81-binding loop sequence is given at the top of the panel.
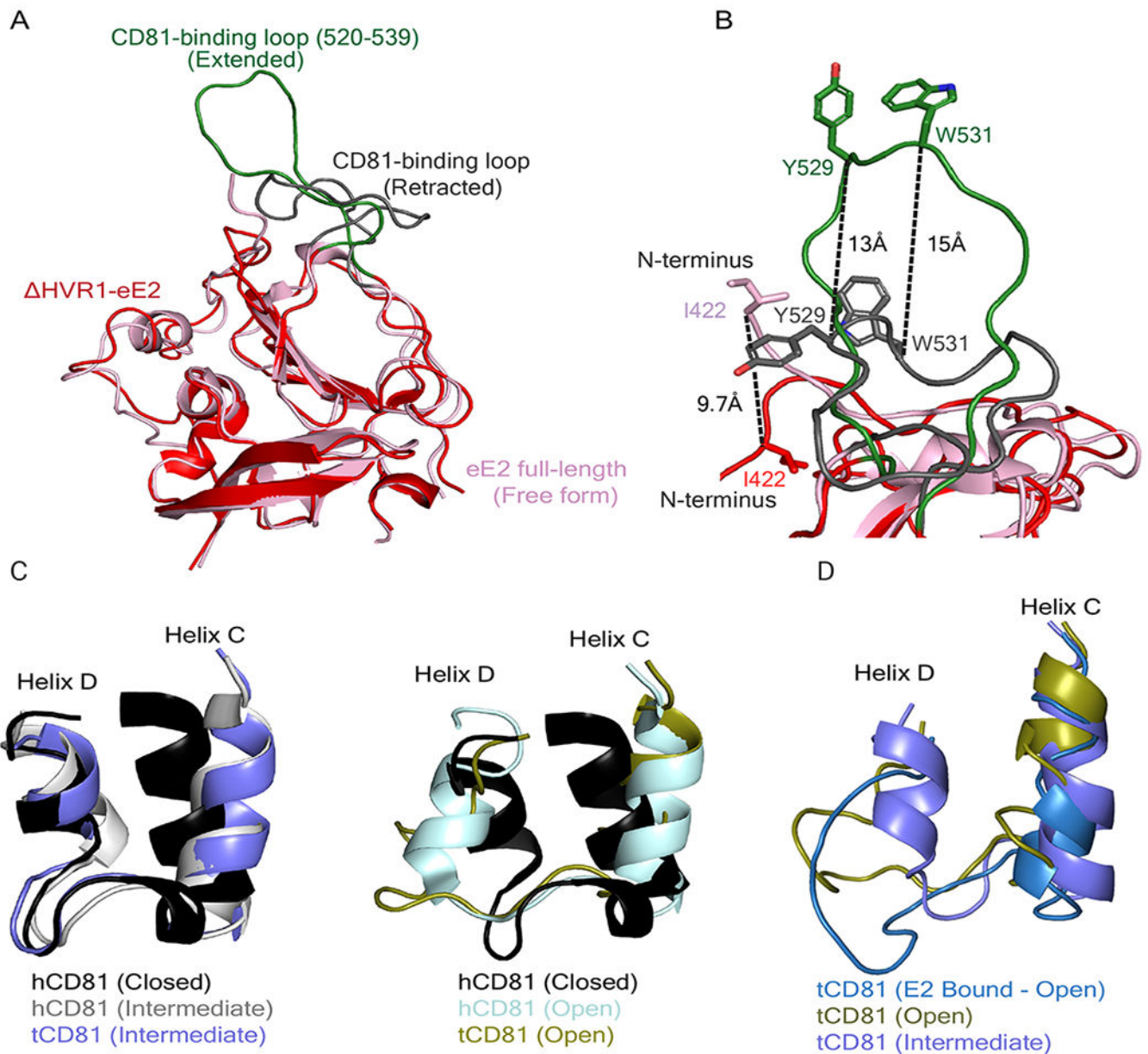
Figure 2: Ribbon diagrams of the conformational variation in E2 and CD81-LEL.
(A and B) Superposition of eE2 in the presence (red/green) and absence (pink/gray) of tCD81-LEL. The CD81-binding loops (residues 520-539) in the presence (green) and absence (gray) of tCD81-LEL, (B) relative alpha carbon movement (dotted lines) of Ile422, Tyr529, and Trp531 side chains (sticks), and N-termini are labeled. (C) Superposition of the unbound C and D helices of tCD81-LEL (violet and olive) and hCD81-LEL (PDB ID 5M2C and 5M33 show the black, light gray, and aqua in the closed, intermediate and open conformations, respectively). (D) Superposition of tCD81-LEL unbound intermediate (violet) and open (olive) conformations with the open E2-bound conformation (blue).
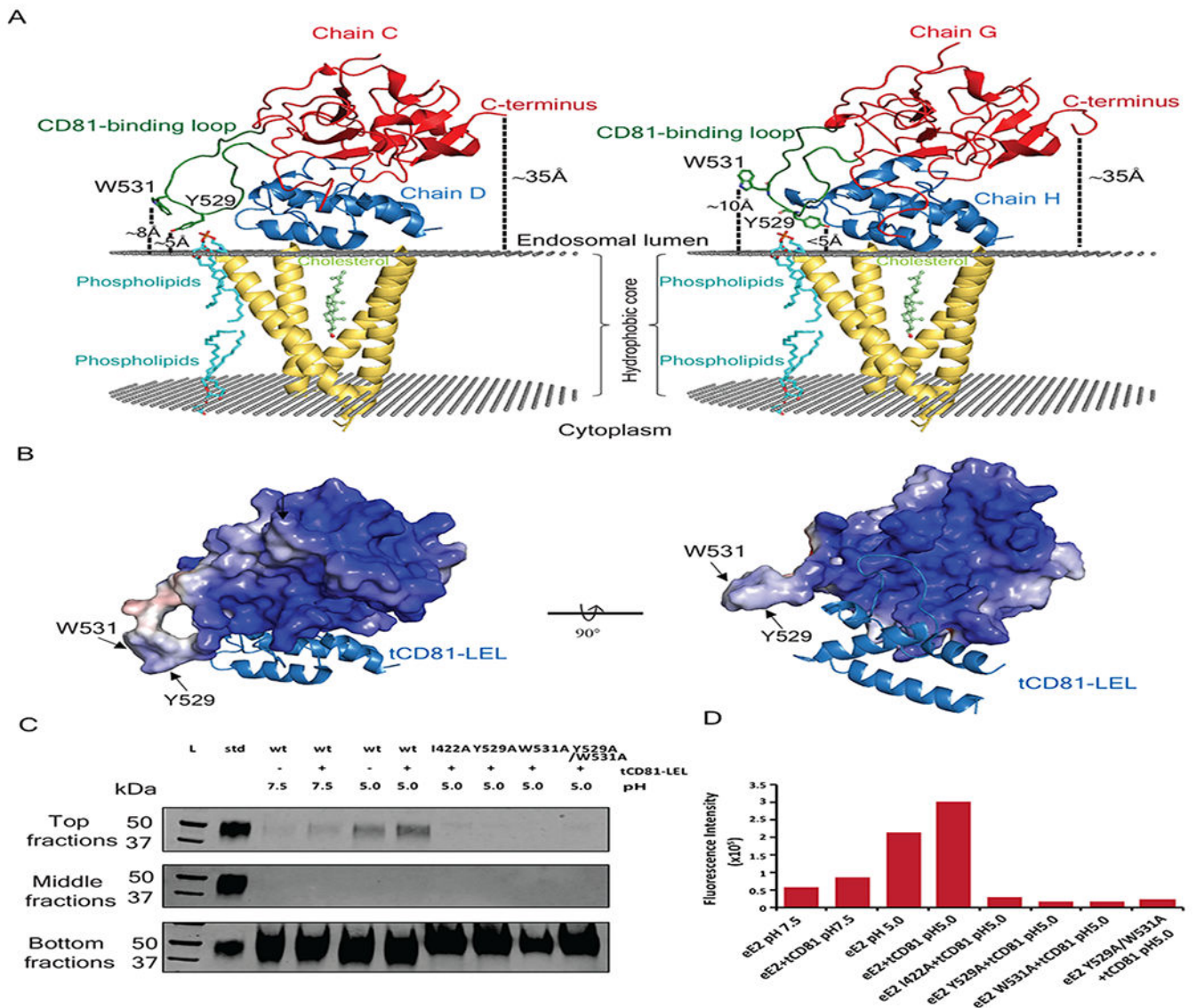
Figure 3: Neutralizing antibodies compete directly with CD81 for E2 binding.
(A) Antibody footprints, colored as in key, mapped onto surface rendering (light gray) of HVR1-eE2 relative to tCD81 (transparent blue ribbon diagram). The right panel is rotated 90° about a vertical axis relative to the left panel. (B) Antibody-binding regions (dashed line, labeled) that compete for the CD81-LEL footprint (blue) on surface rendered (light gray) HVR1-eE2. Asterisks denote antibodies sharing common regions on Fabs antigenic regions (ARs) and antigenic site (AS) 435. (C) Superimposed ribbon diagrams of the E2 front and back layers from chain C (red) of the tCD81-LEL/ HVR1-eE2/2A12 complex with the CD81-binding loop in green and eE2 free from (dark gray) with various E2/Fab complexes (PDB IDs 6MEI, 6MEH, 6BKC, 6URH, 4WEB, 4MWF, 6BKD, and 6BKB are colored light gray).
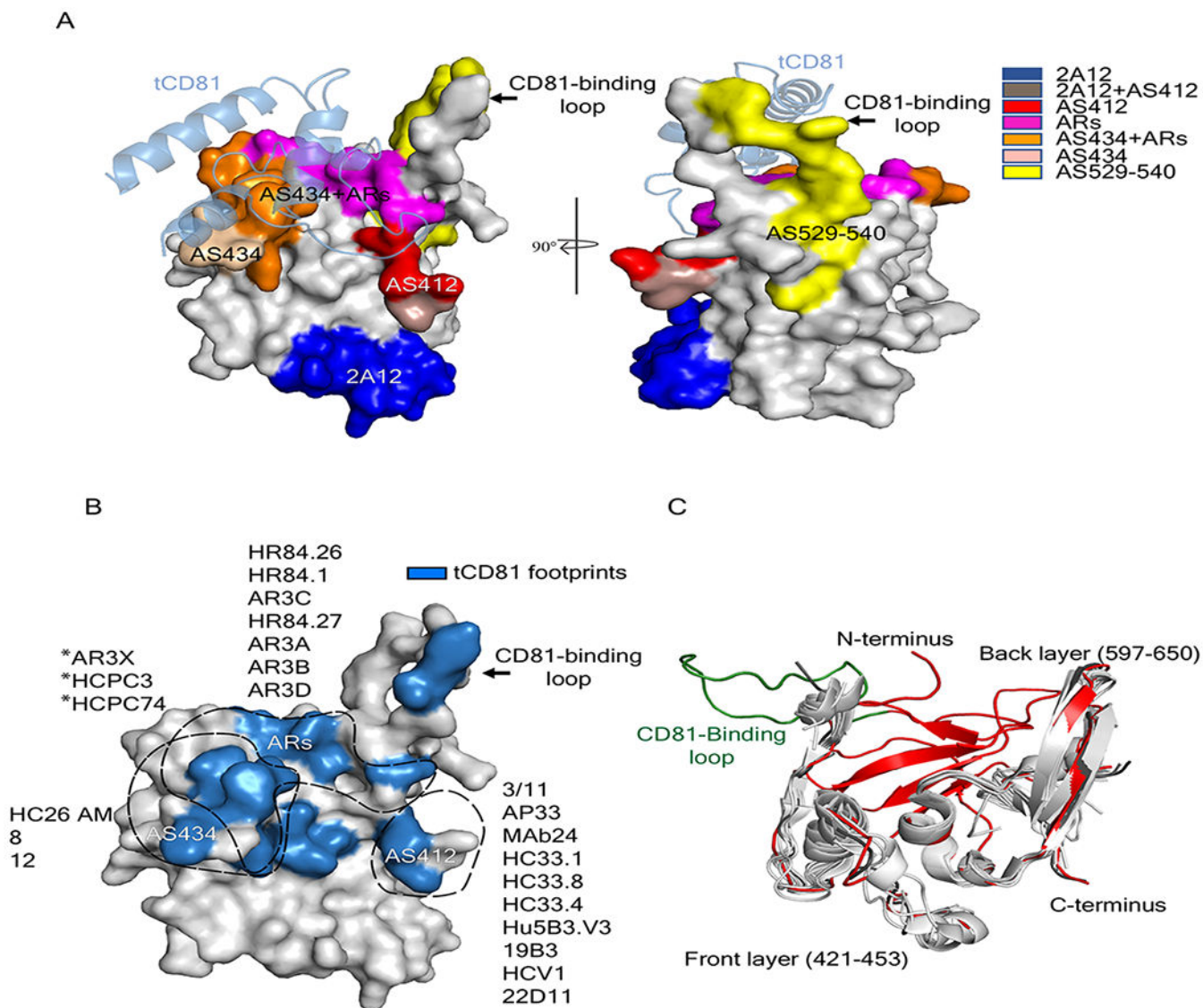
Figure 4: Proximity and interaction of eE2 with membranes.
(A) The full-length human CD81 structure (ribbon diagram and TMs in yellow) and coordinated cholesterol molecule (light green heteroatom sticks) (PDB ID 5TCX) were docked into an idealized POPC membrane bilayer. Parallel planes of gray spheres represent the carbonyl moieties that define the hydrophobic core, and representative phospholipids (cyan heteroatom sticks) are shown. Ribbon diagrams of each tCD81-LEL (blue)/ HVR1-eE2 (red) complex (CD81-binding loop green) in the asymmetric unit are superimposed on the LEL and are shown in the same orientation. Relative distances (dotted lines) of Tyr529 and Trp531 (green heteroatom sticks) and of the carboxyl terminus of HVR1-eE2 from the hydrophobic membrane core are labeled. (B) Electrostatic surface of HVR1-eE2 bound to tCD81-LEL (blue ribbon diagram) calculated at pH 5.0 in the same orientation as A (left) and rotated 90° about a horizontal axis (right) to show membrane-proximal surface. The surface is colored by electrostatic potential corresponding to +5 kcal/(mol·e) (blue) and −5 kcal/(mol·e) (red). (C) E2-specific Western blots of top, middle, and bottom

fractions from liposome flotation in sucrose gradients with protein molecular weight marker (L) and eE2 loading control marker (std). One representative Western blot is shown from three independent experiments. Each experiment demonstrated the same trend, i.e. enhanced floatation of eE2 in the presence of tCD81-LEL and low pH. For gel source data, see Supplementary Information Figure 1. (D) Quantitation of the top fraction Western blot in panel C with arbitrary units. (C and D) The pH, inclusion of tCD81-LEL, and eE2 wild-type (wt) and mutants are labeled.